2011 American Control Conference
on O'Farrell Street, San Francisco, CA, USA
June 29 - July 01, 2011

# Real-Time Automotive Slip Angle Estimation with Nonlinear Observer

G. Phanomchoeng[1], R. Rajamani[1] and D. Piyabongkarn[2]

*Abstract*— **This paper utilizes a new nonlinear observer design technique for estimation of slip angle in automotive applications. Inexpensive sensors that measure yaw rate and lateral acceleration and are normally available for yaw stability control systems are used. The observer design approach utilizes the mean value theorem to express the nonlinear error dynamics as a convex combination of known matrices with time varying coefficients. A modified form of the mean value theorem for vector nonlinear systems is presented. The observer gains are then obtained by solving linear matrix inequalities (LMIs). The developed approach also can enable observer design for a large class of differentiable nonlinear systems with a globally (or locally) bounded Jacobian. The developed nonlinear observer is evaluated through experimental tests on a Volvo XC90 sport utility vehicle. Detailed experimental results show that the developed nonlinear observer can reliably estimate slip angle for a variety of test maneuvers on road surfaces with different friction coefficients.**

## I. Introduction

Electronic stability control (ESC) systems that prevent vehicles from spinning, drifting out, and rolling over have been developed and recently commercialized by several automotive manufacturers [1],[2],[3]. Many electronic stability control systems focus on yaw rate feedback for enhancing stability performance. In such cases, the control system attempts to ensure that the actual yaw rate of the vehicle tracks a desired yaw rate determined by the driver's steering input [1]. However, in situations on low-friction road surfaces, it is also beneficial to control the vehicle slip angle and prevent it from becoming too large, in addition to controlling yaw rate [1],[2],[3]. Slip angle control is necessary because too high a slip angle can reduce the ability of the tires to generate lateral forces and can significantly compromise the performance of the vehicle control system. Hence, both yaw rate and slip angle are variables needed for vehicle stability control.

This paper focuses on slip angle estimation using a nonlinear observer design technique. To begin with, let us review the formal definition of slip angle. The slip angle of a vehicle $\beta$ is the angle its velocity vector at the center of gravity (c.g.) makes with the longitudinal axis of the vehicle. The slip angle of a tire $\alpha$ is the angle of the velocity vector at the tire with the orientation of the tire [1]. Both of these definitions are illustrated in Figure 1.

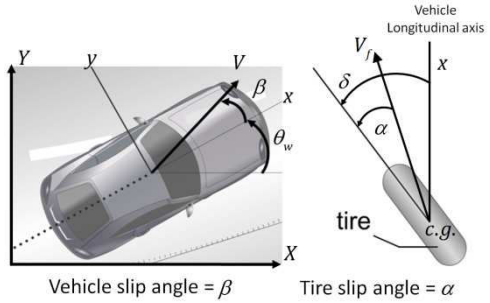


Figure 1 Vehicle and tire slip angles.

## II. Review of Slip Angle Estimation Methods

### A. Slip Angle Measurement Sensors

A one-antenna GPS system can measure the global orientation of the velocity vector of the vehicle, but cannot measure slip angle, since orientation of the vehicle itself cannot be measured. However, several researchers have developed systems for slip angle measurement based on the use of an inertial measurement unit together with a one-antenna GPS system [4]. The major problem with this integration approach is that bias errors in the acceleration measurements will cause drift in the velocity estimates. Another disadvantage of GPS-based systems in general is that they are unreliable in urban environments where tall buildings and urban canyons can prevent access to GPS satellite signals. A two-antenna GPS system can be used to obtain absolute orientation of the vehicle [5], [6] and to correct for bias errors [5]. However, two-antenna GPS systems are likely to cost at least $600 and will be considered expensive for passenger sedans by automotive manufacturers.

Noncontact optical sensors for slip angle measurement have been developed by Corrsys–Datron [7] and others. These sensors use optical means to capture planar road texture and evaluate the motion of the vehicle by measuring the direction and magnitude of change with respect to the road texture. Such optical sensors can provide very accurate slip angle measurements. However, they are very expensive.

### B. Dynamic Model-Based Estimation

A more cost-effective solution compared with optical sensors and GPS-based systems is to estimate slip angle from typical on-board sensors already available for use by the vehicle stability control system. For example, accelerometers, a gyroscope, and a steering angle sensor are typically used by all stability control systems. Several

[1]G. Phanomchoeng and R. Rajamani are with the University of Minnesota, Minneapolis, MN 55455, Email: rajamani@me.umn.edu, TEL 612-626-7961.

[2]D. Piyabongkarn is with the Innovation Center, Eaton Corporation, Eden Prairie, MN55344 USA, E-mail: nengpiyabongkarn@eaton.com.

researchers have proposed different slip angle estimation methodologies based on use of the above stability control system sensors. Most methods can be categorized in two groups: kinematics-based methods [2], [3], [8] and vehicle-model-based methods [9], [10], [11]. The kinematics-based methods (or integration methods) are robust against vehicle parameters, changes in tire-road conditions, and changes in driving maneuvers. However, such methods are very sensitive to sensor error, especially sensor bias error which causes a drift. The model-based methods, on the other hand, are relatively robust against sensor errors. However, they depend heavily on the accuracy of the vehicle and tire parameters and knowledge of road conditions. Most slip angle estimation methods rely on a linear vehicle model that can work effectively only under nominal vehicle operating conditions. When the vehicle is skidding and the slip angle becomes large, these estimation methods no longer work reliably.

In this paper, we present a method of estimating vehicle slip angle based on a nonlinear vehicle model. The method is suitable for a large range of operating conditions. The developed estimation algorithm was validated with experimental measurements on a test vehicle. It was verified that this slip angle estimation provides reliable slip angle under varying road conditions.

## III. Nonlinear Observer Design

### *3.1 Problem Statement*

This section presents an efficient methodology for designing observers for the class of nonlinear systems described by

$$\begin{aligned} \dot{x} &= Ax + \Phi(x) + g(y,u) \\ y &= Cx + \Psi(x) \end{aligned} \tag{1}$$

where $x \in R^n$ is the state vector, $u \in R^p$ is the input vector, and $y \in R^m$ is the output measurement vector. $A \in R^{n\times n}$ and $C \in R^{m\times n}$ are appropriate matrices. The functions $\Phi(x)\colon R^n \to R^n$, $\Psi(x)\colon R^n \to R^m$, and $g(y,u)\colon R^m \times R^p \to R^n$ are nonlinear. In addition, $\Phi(x)$ and $\Psi(x)$ are assumed to be differentiable.

The observer will be assumed to be of the form

$$\begin{aligned} \dot{\hat{x}} &= A\hat{x} + \Phi(\hat{x}) + g(y,u) + L(y - \hat{y}) \\ \hat{y} &= C\hat{x} + \Psi(\hat{x}). \end{aligned} \tag{2}$$

The estimation error dynamics are then seen to be given by

$$\dot{\tilde{x}} = (A - LC)\tilde{x} + \tilde{\Phi} - L\tilde{\Psi} \tag{3}$$

where $\tilde{x} = x - \hat{x}$, $\tilde{\Phi} = \Phi(x) - \Phi(\hat{x})$, and $\tilde{\Psi} = \Psi(x) - \Psi(\hat{x})$.

Let the Lyapunov function candidate for observer design be defined as $V = \tilde{x}^T P\tilde{x}$ where $P > 0$ and $P \in R^{n\times n}$. Then, its derivative is

$$\begin{aligned} \dot{V} = \tilde{x}^T[(A - LC)^T P + P(A - LC)]\tilde{x} \\ +\tilde{x}^T P\tilde{\Phi} + \tilde{\Phi}^{\mathrm{T}} P\tilde{x} - \tilde{x}^T PL\tilde{\Psi} - \tilde{\Psi}^{\mathrm{T}} L^T P\tilde{x}. \end{aligned} \tag{4}$$

### *3.2 Mean Value Theorem for Bounded Jacobian Systems*

In this section, we present a mathematical tool which is used subsequently to develop the observer gain in the next section. First, we present the scalar mean value theorem and the mean value theorem for vector functions. Then, we define the canonical basis for writing a vector function with a composition form. Lastly, we present a new modified form of the mean value theorem for vector functions.

**Lemma 1:** Scalar Mean Value Theorem

Let $f(x)\colon R \to R$ be a function continuous on $[a,b] \subset R$ and differentiable on $(a,b)$. For $x_1,\ x_2 \in [a,b]$, there exists $c \in (a,b)$ such that

$$f(x_2) - f(x_1) = \left.\frac{df}{dx}\right|_{x=c} \times (x_2 - x_1). \tag{5}$$

The equation (5) can also be rewritten as

$$\begin{aligned} f(x_2) - f(x_1) = \left(\delta_1 \left.\frac{df}{dx}\right|_{x=c_1} + \delta_2 \left.\frac{df}{dx}\right|_{x=c_2}\right)(x_2 - x_1), \\ \delta_1, \delta_2 > 0,\ \ \delta_1 + \delta_2 = 1. \end{aligned} \tag{6}$$

where $c_1, c_2 \in (a,b)$ and $\delta_1$and $\delta_2$ are parameters that vary with the value of $x_1$ and $x_2$. The proof of this lemma is available in [12].

**Lemma 2:** Mean Value Theorem for a Vector Function, [13]

Let $f(x)\colon R^n \to R^n$ be a function continuous on $[a,b] \in R^n$ and differentiable on a convex hull of the set $(a,b)$ with a Lipschitz continuous gradient $\nabla f$. For $s_1, s_2 \in [a,b]$, there exists $c \in (a,b)$ such that

$$f(s_2) - f(s_1) = \nabla f(c)(s_2 - s_1). \tag{7}$$

However, we cannot directly use the mean value theorem of equation (7), since $c$ is a varying parameter that continuously changes with the values of $s_1$ and $s_2$. Thus $\nabla f(c)$ is an unknown and changing matrix. We need to modify the mean value theorem before it can be utilized.

**Lemma 3:** Canonical Basis, [14]

Let the canonical basis of the vectorial space $R^s$ for all $s \geq 1$ be defined by:

$$E_s = \{e_s(i) | e_s(i) = (0,\dots,0,1,0,\dots,0)^T, i = 1,\dots,s\}. \tag{8}$$

Let a vector function be defined by $f(x)\colon R^n \to R^q$. Then, $f(x) = \left[f_1(x),\dots,f_q(x)\right]^T$ where $f_i(x)\colon R^n \to R$ is the i$^{\text{th}}$ component of $f(x)$ and $x \in R^n$. The vectorial space $R^q$ is generated by the canonical basis $E_q$. Therefore, $f(x)$ can be written as:

$$f(x) = \sum_{i=1}^{q} e_q(i) f_i(x). \tag{9}$$

Now, we are ready to state and prove a modified form of the mean value theorem for a vector function.

**Theorem 1:** Modified Mean Value Theorem for a Vector Function

Let $f(x)\colon R^n \to R^n$ be a function continuous on $[a,b] \in R^n$ and differentiable on convex hull of the set $(a,b)$. For $s_1, s_2 \in [a,b]$, there exist $\delta_{ij}^{max}$ and $\delta_{ij}^{min}$ for $i = 1,\dots,n$ and $j = 1,\dots,n$ such that:

$$\begin{aligned} f(s_2) - f(s_1) = \left[\left(\sum_{i,j=1}^{n,n} H_{ij}^{max}\delta_{ij}^{max}\right) + \left(\sum_{i,j=1}^{n,n} H_{ij}^{min}\delta_{ij}^{min}\right)\right](s_2 - s_1), \\ \delta_{ij}^{max}, \delta_{ij}^{min} \geq 0, \quad \delta_{ij}^{max} + \delta_{ij}^{min} = 1 \end{aligned} \tag{10}$$

where 1) $h_{ij}^{max} \geq max\left(\partial f_i/\partial x_j\right)$ and $h_{ij}^{min} \leq min\left(\partial f_i/\partial x_j\right)$ 2) $H_{ij}^{max} = e_n(i)e_n^T(j)h_{ij}^{max}$and $H_{ij}^{min} = e_n(i)e_n^T(j)h_{ij}^{min}$. The proof of theorem 1 is in the appendix.

*Illustrative Example for Theorem 1*

The following is a 2 dimensional example of the

application of the mean value theorem for a higher-dimensional function. Let $f(s)\colon R^2 \to R^2$ be define by:

$$f(s) = [f_1(s) \quad f_2(s)]^T \tag{11}$$

If we set $s_1 = [s_{11}, s_{12}]^T$ and $s_2 = [s_{21}, s_{22}]^T$, then

$$f(s_2) - f(s_1) = \nabla f(c)(s_2 - s_1) =$$

$$\begin{bmatrix} \begin{bmatrix} max\left(\frac{\partial f_1}{\partial x_1}\right) & 0 \\ 0 & 0 \end{bmatrix} \delta_{11}^{max} + \begin{bmatrix} min\left(\frac{\partial f_1}{\partial x_1}\right) & 0 \\ 0 & 0 \end{bmatrix} \delta_{11}^{min} \\ + \begin{bmatrix} 0 & max\left(\frac{\partial f_1}{\partial x_2}\right) \\ 0 & 0 \end{bmatrix} \delta_{12}^{max} + \begin{bmatrix} 0 & min\left(\frac{\partial f_1}{\partial x_2}\right) \\ 0 & 0 \end{bmatrix} \delta_{12}^{min} \\ + \begin{bmatrix} 0 & 0 \\ max\left(\frac{\partial f_2}{\partial x_1}\right) & 0 \end{bmatrix} \delta_{21}^{max} + \begin{bmatrix} 0 & 0 \\ min\left(\frac{\partial f_2}{\partial x_1}\right) & 0 \end{bmatrix} \delta_{21}^{min} \\ + \begin{bmatrix} 0 & 0 \\ 0 & max\left(\frac{\partial f_2}{\partial x_2}\right) \end{bmatrix} \delta_{22}^{max} + \begin{bmatrix} 0 & 0 \\ 0 & min\left(\frac{\partial f_2}{\partial x_2}\right) \end{bmatrix} \delta_{22}^{min} \end{bmatrix} \times \left( \begin{bmatrix} s_{21} \\ s_{22} \end{bmatrix} - \begin{bmatrix} s_{11} \\ s_{12} \end{bmatrix} \right) \tag{12}$$

or

$$f(s_2) - f(s_1) = \begin{bmatrix} H_{11}^{max}\delta_{11}^{max} + H_{11}^{min}\delta_{11}^{min} \\ +H_{12}^{max}\delta_{12}^{max} + H_{12}^{min}\delta_{12}^{min} \\ +H_{21}^{max}\delta_{21}^{max} + H_{21}^{min}\delta_{21}^{min} \\ +H_{22}^{max}\delta_{22}^{max} + H_{22}^{min}\delta_{22}^{min} \end{bmatrix} \times \left( \begin{bmatrix} s_{21} \\ s_{22} \end{bmatrix} - \begin{bmatrix} s_{11} \\ s_{12} \end{bmatrix} \right), \tag{13}$$

$$\delta_{ij}^{max}, \delta_{ij}^{min} \geq 0, \qquad \delta_{ij}^{max} + \delta_{ij}^{min} = 1$$

where $H_{ij}^{max} = e_n(i)e_n^T(j)h_{ij}^{max}$, $H_{ij}^{min} = e_n(i)e_n^T(j)h_{ij}^{min}$, and $h_{ij}^{max} \geq max\left(\partial f_i/\partial x_j\right)$ and $h_{ij}^{min} \leq min\left(\partial f_i/\partial x_j\right)$.

### *3.3 Nonlinear Observer*

**Theorem 2:** Bounded Jacobian Observer for General Problem

For the class of systems and observer forms described in equations (1) and (2), if an observer gain matrix $L$ can be chosen such that

$$\begin{gathered} P\left(A + \bar{H}_{ij}^{max}\right) + \left(A + \bar{H}_{ij}^{max}\right)^T P - \left(C + \bar{G}_{kj}^{max}\right)^T L^T P - PL\left(C + \bar{G}_{kj}^{max}\right) < 0 \\ P\left(A + \bar{H}_{ij}^{max}\right) + \left(A + \bar{H}_{ij}^{max}\right)^T P - \left(C + \bar{G}_{kj}^{min}\right)^T L^T P - PL\left(C + \bar{G}_{kj}^{min}\right) < 0 \\ P\left(A + \bar{H}_{ij}^{min}\right) + \left(A + \bar{H}_{ij}^{min}\right)^T P - \left(C + \bar{G}_{kj}^{max}\right)^T L^T P - PL\left(C + \bar{G}_{kj}^{max}\right) < 0 \\ P\left(A + \bar{H}_{ij}^{min}\right) + \left(A + \bar{H}_{ij}^{min}\right)^T P - \left(C + \bar{G}_{kj}^{min}\right)^T L^T P - PL\left(C + \bar{G}_{kj}^{min}\right) < 0 \\ P > 0 \end{gathered} \tag{14}$$

$$\forall i = 1, \dots, n\,, \forall j = 1, \dots, n \text{ and } \forall k = 1, \dots, m,$$

where

1) $h_{ij}^{max} \geq max\left(\partial\Phi_i/\partial x_j\right)$ and $h_{ij}^{min} \leq min\left(\partial\Phi_i/\partial x_j\right)$,
2) $H_{ij}^{max} = e_n(i)e_n^T(j)h_{ij}^{max}$ and $H_{ij}^{min} = e_n(i)e_n^T(j)h_{ij}^{min}$,
3) $z_H = n \times n$ is the state scaling factor, $n$ being dimension of the state vector,
4) $\bar{H}_{ij}^{max} = z_H H_{ij}^{max}$ and $\bar{H}_{ij}^{min} = z_H H_{ij}^{min}$,
5) $g_{kj}^{max} \geq max\left(\partial\Psi_k/\partial x_j\right)$ and $g_{kj}^{min} \leq min\left(\partial\Psi_k/\partial x_j\right)$,
6) $G_{kj}^{max} = e_n(k)e_n^T(j)g_{kj}^{max}$ and $G_{kj}^{min} = e_n(k)e_n^T(j)g_{kj}^{min}$,
7) $z_G = m \times n$ is the output scaling factor, $m$ being dimension of the output vector,
8) $\bar{G}_{kj}^{max} = z_G G_{kj}^{max}$ and $\bar{G}_{kj}^{min} = z_G G_{kj}^{min}$,

then this choice of $L$ leads to asymptotically stable estimates by the observer (2) for the system (1).

The proof of theorem 2 is in the journal version of this paper [17].

**Corollary to Theorem 2**: Bounded Jacobian Observer for Specified Problem

For the class of systems and observer forms described in equations (1) and (2), if an observer gain matrix $L$ can be chosen such that

$$\begin{gathered} P\left(A + \bar{H}_{ij}^{max}\right) + \left(A + \bar{H}_{ij}^{max}\right)^T P - \left(C + \bar{G}_{kj}^{max}\right)^T L^T P - PL\left(C + \bar{G}_{kj}^{max}\right) < 0 \\ P\left(A + \bar{H}_{ij}^{max}\right) + \left(A + \bar{H}_{ij}^{max}\right)^T P - \left(C + \bar{G}_{kj}^{min}\right)^T L^T P - PL\left(C + \bar{G}_{kj}^{min}\right) < 0 \\ P\left(A + \bar{H}_{ij}^{min}\right) + \left(A + \bar{H}_{ij}^{min}\right)^T P - \left(C + \bar{G}_{kj}^{max}\right)^T L^T P - PL\left(C + \bar{G}_{kj}^{max}\right) < 0 \\ P\left(A + \bar{H}_{ij}^{min}\right) + \left(A + \bar{H}_{ij}^{min}\right)^T P - \left(C + \bar{G}_{kj}^{min}\right)^T L^T P - PL\left(C + \bar{G}_{kj}^{min}\right) < 0 \\ P > 0 \end{gathered} \tag{15}$$

$$\forall i = 1, \dots, n\,, \forall j = 1, \dots, n \text{ and } \forall k = 1, \dots, m,$$

where

1) $h_{ij}^{max} \geq max\left(\partial\Phi_i/\partial x_j\right)$ and $h_{ij}^{min} \leq min\left(\partial\Phi_i/\partial x_j\right)$,
2) $H_{ij}^{max} = e_n(i)e_n^T(j)h_{ij}^{max}$ and $H_{ij}^{min} = e_n(i)e_n^T(j)h_{ij}^{min}$,
3) $\bar{z}_H = n \times n - w_H$ is the state scaling factor, $n$ being dimension of the state vector, $w_H$ being the number of terms in $\partial\Phi_i/\partial x_j$ that equals zero,
4) $\bar{H}_{ij}^{max} = \bar{z}_H H_{ij}^{max}$ and $\bar{H}_{ij}^{min} = \bar{z}_H H_{ij}^{min}$,
5) $g_{kj}^{max} \geq max\left(\partial\Psi_k/\partial x_j\right)$ and $g_{kj}^{min} \leq min\left(\partial\Psi_k/\partial x_j\right)$,
6) $G_{kj}^{max} = e_n(k)e_n^T(j)g_{kj}^{max}$ and $G_{kj}^{min} = e_n(k)e_n^T(j)g_{kj}^{min}$,
7) $\bar{z}_G = m \times n - w_G$ is the output scaling factor, $m$ being dimension of the output vector, $w_G$ being the number of terms in $\partial\Psi_k/\partial x_j$ that equals zero,
8) $\bar{G}_{kj}^{max} = \bar{z}_G G_{kj}^{max}$ and $\bar{G}_{kj}^{min} = \bar{z}_G G_{kj}^{min}$,

then this choice of $L$ leads to asymptotically stable estimates by the observer (2) for the system (1).

A proof of the Corollary to Theorem 2 is in the appendix.

## IV. Mathematic Formulation of Slip Angle Estimation Problem

### *4.1 Vehicle Lateral Dynamics*

Consider the two-degrees-of –freedom (2-DOF) model used to represent the vehicle lateral dynamics as shown in Figure 2. The 2 DOF are the lateral translation of the vehicle $y$ and the yaw rate $r$ of the vehicle. The nonlinear vehicle lateral dynamics when the steering angle is assumed to be small can be formulated as

$$ma_y = m(\ddot{y} + ru_x) = F_{yf} + F_{yr} \tag{16}$$

$$I_z\dot{r} = aF_{yf} - bF_{yr} \tag{17}$$

where $F_{yf}$ and $F_{yr}$ are the lateral tire forces of the front and rear wheels respectively, $u_x$ is longitudinal velocity and $a$ and $b$ are the distances of the front and rear tires respectively from the c.g. of the vehicle.

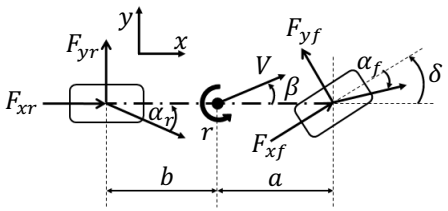


Figure 2 Single track model for vehicle lateral dynamics

It should be noted that in the presence of road bank angle, the lateral translational equation (16) is modified to $m(\ddot{y} + ru_x) = F_{yf} + F_{yr} - mgsin(\varphi_r)$, where $\varphi_r$ is the road bank angle. Since the measured lateral acceleration includes the influence of the gravity component due to the road bank angle, the lateral acceleration measurement is given by $a_y = \ddot{y} + ru_x + gsin(\varphi_r)$. Hence, the equation $ma_y = F_{yf} + F_{yr}$ holds even in the presence of road bank angle. Road bank angle also does not affect equation (17).

The lateral tire force for each of the front and rear tires is computed from a lateral tire model for parabolic normal pressure distribution [1]:

$$F_y = \mu F_z\,(3\theta\alpha - 3\theta^2\alpha^2 sgn(\alpha) + \theta^3\alpha^3),\ \theta = \frac{4a_c^2 b_c k}{3\mu F_z} \quad (18)$$

where $\mu$ is tire-road friction coefficient, $F_z$ is the vertical force on the tire, $a_c$ is half-length of contact patch, $b_c$ is half-width of contact patch, and $k$ is isotropic stiffness of tire elements per unit area of the belt surface. Assume that the variables $\mu, F_z,$ and $\theta$ are known and that they change slowly. This is a reasonable assumption. The variable $\theta$ is indeed a constant dependent only on tire parameters. While the variable $F_z$ does change somewhat with longitudinal acceleration and deceleration, this change is slow and can be estimated quite easily. The friction coefficient $\mu$ can be estimated from the longitudinal dynamics of the vehicle [1], [16]. The equation (18) can then be simplified as

$$F_y = c_1\alpha - c_2\alpha^2 sgn(\alpha) + c_3\alpha^3. \quad (19)$$

Note: It is also possible to use other nonlinear lateral tire models for the problem, such as the Pacejka Magic Formula tire model [1].

The slip angles at the front and rear tires can be related to the body slip angle and the yaw rate using the following linear approximations:

$$\alpha_f = \delta - \left(\beta + \frac{ra}{u_x}\right),\ \alpha_r = \frac{rb}{u_x} - \beta \quad (20)$$

where $\alpha_f$ and $\alpha_r$ are slip angles of the front and rear wheels respectively and $\beta$ is vehicle body slip angle. Including the tire model, the vehicle dynamic model can be written as

$$\begin{aligned} ma_y &= m(\ddot{y} + ru_x) = c_{1f}\alpha_f + c_{1r}\alpha_r + \eta(\alpha_f) + \eta(\alpha_r) \\ I_z\dot{r} &= ac_{1f}\alpha_f - bc_{1r}\alpha_r + a\eta(\alpha_f) - b\eta(\alpha_r) \end{aligned} \quad (21)$$

where $\eta(\alpha_f) = -c_{2f}\alpha_f^2 sgn(\alpha_f) + c_{3f}\alpha_f^3$ and $\eta(\alpha_r) = -c_{2r}\alpha_r^2 sgn(\alpha_r) + c_{3r}\alpha_r^3$.

We need to rewrite equation (21) in the standard system dynamics format described by equation (1). It is possible to choose $\beta$ and $r$ as the state vector and write equation (21) in the form of equation (1). However, the nonlinearities of the system will become too complicated, if these state variables are chosen. To overcome this problem, we choose the slip angles at the front and rear tires $\alpha_f$ and $\alpha_r$ as the states. Then, the system equations can be written as

$$\begin{aligned} \begin{bmatrix}\dot{\alpha}_f \\ \dot{\alpha}_r\end{bmatrix} &= \begin{bmatrix} -\left(\frac{u_x}{a+b} + \frac{a^2c_{1f}}{I_z u_x}\right) & \left(\frac{u_x}{a+b} + \frac{abc_{1r}}{I_z u_x}\right) \\ -\left(\frac{u_x}{a+b} - \frac{abc_{1f}}{I_z u_x}\right) & \left(\frac{u_x}{a+b} - \frac{b^2c_{1r}}{I_z u_x}\right) \end{bmatrix}\begin{bmatrix}\alpha_f \\ \alpha_r\end{bmatrix} \\ &+ \begin{bmatrix} \left(\frac{u_x}{a+b}\right) & 1 & -\frac{1}{u_x} \\ \left(\frac{u_x}{a+b}\right) & 0 & -\frac{1}{u_x} \end{bmatrix}\begin{bmatrix}\delta \\ \dot{\delta} \\ a_y\end{bmatrix} + \begin{bmatrix} -\frac{a^2}{I_z u_x}\eta(\alpha_f) + \frac{ab}{I_z u_x}\eta(\alpha_r) \\ +\frac{ab}{I_z u_x}\eta(\alpha_f) - \frac{b^2}{I_z u_x}\eta(\alpha_r) \end{bmatrix}. \end{aligned} \quad (22)$$

For the output, we can measure $a_y$ using an accelerometer and $r$ by a gyroscope. Also, we know the steering input, $\delta$, and the steering rate input, $\dot{\delta}$. These are known inputs. Then, the output equation can be written as

$$\begin{bmatrix}y_1 \\ y_2\end{bmatrix} = \begin{bmatrix} r - \left(\frac{u_x}{a+b}\right)\delta \\ a_y \end{bmatrix} = \begin{bmatrix} -\left(\frac{u_x}{a+b}\right) & \left(\frac{u_x}{a+b}\right) \\ \frac{c_{1f}}{m} & \frac{c_{1r}}{m} \end{bmatrix}\begin{bmatrix}\alpha_f \\ \alpha_r\end{bmatrix} + \begin{bmatrix} 0 \\ \frac{\eta(\alpha_f)}{m} + \frac{\eta(\alpha_r)}{m} \end{bmatrix}. \quad (23)$$

Then, the slip angle of the vehicle can be computed from the slips angles of the front and rear tires as

$$\beta = \delta - \left(\alpha_f + \frac{ra}{u_x}\right) \text{ or } \beta = \frac{rb}{u_x} - \alpha_r. \quad (24)$$

It is desired to use a nonlinear observer based on the above nonlinear vehicle model to estimate slip angle. We use the observer results developed in section 3 to design the nonlinear observer.

### *4.2 Observer Design for Slip Angle Estimation*

For the dynamic equations, the scaling factor $\bar{z}_H$ is 4. ($\bar{z}_H = n \times n - w_H = 2 \times 2 - 0 = 4$). The term $\Phi(x)$ is

$$\Phi(x) = \begin{bmatrix} -\frac{a^2}{I_z u_x}\eta(\alpha_f) + \frac{ab}{I_z u_x}\eta(\alpha_r) \\ +\frac{ab}{I_z u_x}\eta(\alpha_f) - \frac{b^2}{I_z u_x}\eta(\alpha_r) \end{bmatrix} \quad (25)$$

where $\eta(\alpha_f) = -c_{2f}\alpha_f^2 sgn(\alpha_f) + c_{3f}\alpha_f^3$ and $\eta(\alpha_r) = -c_{2r}\alpha_r^2 sgn(\alpha_r) + c_{3r}\alpha_r^3$.

The jacobian of the nonlinear function $\Phi(x)$ is computed to find $\bar{H}_{ij}^{max}$ and $\bar{H}_{ij}^{min}$.

For the measurement equation, the scaling factor $\bar{z}_G$ is 2. Since $\Psi_1(x) = 0$, the scaling factor $\bar{z}_G$ is less than $m \times n$. ($\bar{z}_G = 2 \times 2 - 2 = 2$). The nonlinear function $\Psi(x)$ is

$$\Psi(x) = \begin{bmatrix} 0 & \frac{\eta(\alpha_f)}{m} + \frac{\eta(\alpha_r)}{m} \end{bmatrix}^T. \quad (26)$$

The jacobian of the nonlinear function $\Psi(x)$ is computed to find $\bar{G}_{kj}^{max}$ and $\bar{G}_{kj}^{min}$.

Next, we solve equations (15) for the observer gain. Using the LMI toolbox in Matlab, the example of observer gain for high friction surface is found to be $L = \begin{bmatrix} -40.8224 & 1.6749 \\ 44.9540 & 2.9837 \end{bmatrix}$. (Note: The LMI toolbox in Matlab provides only one gain, though theoretically many solutions can exist to the LMI (15). If a faster convergence rate is desired, the RHS in equation (15) could be replaced by a negative definite matrix instead of zero.)

## V. Experimental Set Up

The test vehicle used for the experimental evaluation is a Volvo XC90 sport utility vehicle. Vehicle testing was conducted at the Eaton Proving Ground in Marshall, Michigan. A MicroAutoBox from dSPACE was used for real-time data acquisition. A real-time GPS system, RT3000, from Oxford Technical Solutions was used for these tests to accurately measure the vehicle slip angle for comparison with the performance of the slip angle estimation algorithm. The specification of slip angle estimates from this system according to the manufacturer is 0.15 degrees [15]. The GPS outputs were connected to the MicroAutoBox via CAN communication at the baud rate of 0.5 Mbits/sec. To obtain objective test results, the vehicle was instrumented to record the relevant values from both CAN network and GPS. The sampling time is set at 2 milliseconds. A photograph of the test vehicle is shown in Figure 3.

The signals required by the observer (2) are the lateral acceleration, longitudinal velocity, yaw rate, steering angle and steering rate. The steering angle was obtained over the CAN network bus of the Volvo XC90. The steering rate was obtained by differentiating the steering angle. The other

variables were obtained from the RT3000 system. While the RT3000 system is an expensive 6 axis inertial system combined with GPS, the observer developed in this paper utilized only raw lateral acceleration, longitudinal velocity and yaw rate signals.

Figure 3 The Volvo XC90 test vehicle with GPS system

## VI. Experimental Evaluation of Slip Angle Estimation

The estimated slip angle was compared with the slip angle measured using the accurate GPS-INS system. Figure 4 shows the experimental results of a double lane-change maneuver on a high friction road with the vehicle speed at 70 mph. The figure shows that the estimated slip angle is able to match the slip angle obtained from the GPS system very well. Figure 5 shows the experimental results of a random driving maneuver on a high friction road surface. It can be seen again that the nonlinear observer provides accurate and drift-free estimates of the slip angle.

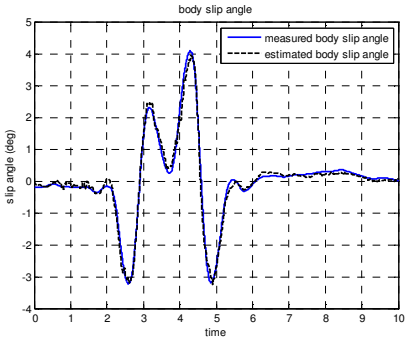


Figure 4 Slip angle estimation result in double lane change test on high friction road surface

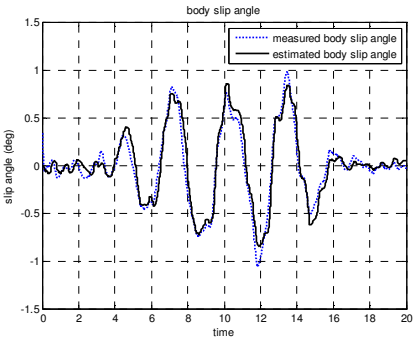


Figure 5 Slip angle estimation result in random driving test

Figures 6 and 7 show the experimental results of a double lane-change maneuver on a low friction road surface ( $\mu = 0.35$) with the vehicle speed at 35 mph. Figure 6 shows the relation between rear slip angle and total lateral force of the vehicle. The figure indicates that the total lateral force is proportional to the slip angle when the slip angle is small ($\alpha < 0.07$). The maximum lateral force is 9000 N. After $\alpha \geq 0.07$, the lateral fire force saturates. In this case, it implies that a linear tire force model cannot be used for this problem. If the model is described by a linear tire force model, it will cause large errors in the slip angle estimation. Figure 7 shows the estimated slip angle on the low friction road.

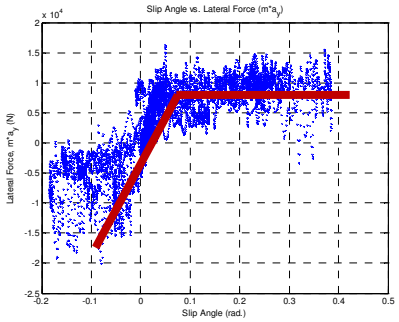


Figure 6 Rear Slip Angle vs. Total Lateral Force ($ma_y$) result in double lane change test on low friction road surface

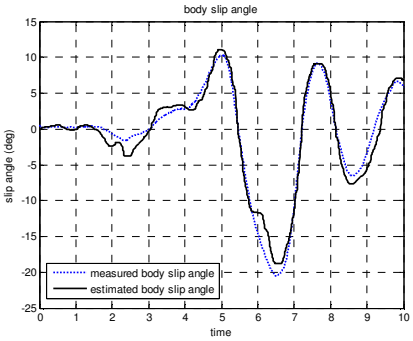


Figure 7 Slip angle estimation result in double lane change test on low friction road surface

The estimation errors for slip angle in the 3 different maneuvers are shown in Table 1. The table shows that the RMS errors are less than 0.15 degrees on high friction road and approximately 1.4 degrees on icy road. It should be noted that the slip angle values are far higher on the icy road and hence the RMS error as a percentage of slip angle range is of the same order as on the high friction road.

Table 1 Estimation Errors for Experimental Tests

| | Double lane-change on high friction surface | Random driving on high friction surface | Double lane-change on low friction surface |
|---|---|---|---|
| Maximum error (deg) | 0.6588 | 0.3791 | 4.7024 |
| RMS error (deg) | 0.1421 | 0.1015 | 1.3217 |
| $\frac{maximum\ error}{maximum\ \beta}$ | 0.1624 | 0.3602 | 0.2273 |
| $R^2$ | 0.98700 | 0.9259 | 0.9662 |

## VII. Conclusion

This paper developed a new nonlinear observer design technique for estimation of slip angle using inexpensive sensors normally available for yaw stability control applications. The approach utilized is to use the mean value theorem to express the nonlinear error dynamics as a convex combination of known matrices with time varying coefficients. The observer gains are then obtained by solving linear matrix inequalities (LMIs). The developed approach can enable observer design for a large class of differentiable nonlinear systems with a globally (or locally) bounded

Jacobian. The developed nonlinear observer for slip angle estimation is evaluated through experimental tests on a Volvo XC90 sport utility. The experimental results show that the developed nonlinear observer can reliably estimate slip angle for a variety of test maneuvers.

## APPENDIX

**The Proof of Theorem 1:** Lemma 2 shows that

$$f(s_2) - f(s_1) = \nabla f(c)(s_2 - s_1) = \begin{bmatrix} \partial f_1/\partial x_1 & \partial f_1/\partial x_2 & \dots & \partial f_1/\partial x_n \\ \partial f_2/\partial x_1 & \partial f_2/\partial x_2 & \dots & \partial f_2/\partial x_n \\ \vdots & \vdots & \vdots & \vdots \\ \partial f_n/\partial x_1 & \partial f_n/\partial x_2 & \dots & \partial f_n/\partial x_n \end{bmatrix}([s_2 - s_1]). \quad (27)$$

Lemma 1 shows that each derivative function can be replaced with a convex combination of 2 values of the derivative of the function. Hence, the derivative function, $\partial f_i(c)/\partial x_j$, can be replaced with

$$\frac{\partial f_i}{\partial x_j}(c) = \delta_{ij}^{max}\frac{\partial f_i}{\partial x_j}(\Omega) + \delta_{ij}^{min}\frac{\partial f_i}{\partial x_j}(\lambda), \quad \delta_{ij}^{max}, \delta_{ij}^{min} \geq 0,\ \delta_{ij}^{max} + \delta_{ij}^{min} = 1 \quad (28)$$

where $\Omega = (\Omega_1, \Omega_2, \dots, \Omega_n)$ and $\lambda = (\lambda_1, \lambda_2, \dots, \lambda_n)$. $c, \Omega_n, \lambda_n \in (a, b)$

To satisfy lemma 1, the values of $\partial f_i(\Omega)/\partial x_j$ and $\partial f_i(\lambda)/\partial x_j$ need to be chosen such that

$$\frac{\partial f_i}{\partial x_j}(\Omega) = h_{ij}^{max} \geq max\left(\frac{\partial f_i}{\partial x_j}\right), \text{and } \frac{\partial f_i}{\partial x_j}(\lambda) = h_{ij}^{min} \leq min\left(\frac{\partial f_i}{\partial x_j}\right). \quad (29)$$

Note: One can easily show that if either $h_{ij}^{max} < max(df_i/dx_j)$ or $h_{ij}^{min} > min(df_i/dx_j)$ for $\forall x \in (a, b)$, then there are no $\delta_{ij}^{max}$and $\delta_{ij}^{min}$ that will satisfy equation (25) with the constraints $\delta_{ij}^{max}, \delta_{ij}^{min} \geq 0$ and $\delta_{ij}^{max} + \delta_{ij}^{min} = 1$.

Then, the equation (28) can be rewritten as

$$\frac{\partial f_i}{\partial x_j}(c) = \delta_{ij}^{max}h_{ij}^{max} + \delta_{ij}^{min}h_{ij}^{min}, \quad \delta_{ij}^{max}, \delta_{ij}^{min} \geq 0,\ \delta_{ij}^{max} + \delta_{ij}^{min} = 1 \quad (30)$$

where $h_{ij}^{max} \geq max(\partial f_i/\partial x_j)$ and $h_{ij}^{min} \leq min(\partial f_i/\partial x_j)$. Note: $\delta_{ij}^{max}, \delta_{ij}^{min}$ are parameters that vary with the value of $s_1$ and $s_2$. Hence, the equation (27) can be rewritten as

$$f(s_2) - f(s_1) = \begin{bmatrix} \delta_{11}^{max}h_{11}^{max} & \delta_{12}^{max}h_{12}^{max} & \dots & \delta_{1n}^{max}h_{1n}^{max} \\ \delta_{21}^{max}h_{21}^{max} & \delta_{22}^{max}h_{22}^{max} & \dots & \delta_{2n}^{max}h_{2n}^{max} \\ \vdots & \vdots & \vdots & \vdots \\ \delta_{n1}^{max}h_{n1}^{max} & \delta_{n2}^{max}h_{n2}^{max} & \dots & \delta_{nn}^{max}h_{nn}^{max} \end{bmatrix}([s_2 - s_1]) + \begin{bmatrix} \delta_{11}^{min}h_{11}^{min} & \delta_{12}^{min}h_{12}^{min} & \dots & \delta_{1n}^{min}h_{1n}^{min} \\ \delta_{21}^{min}h_{21}^{min} & \delta_{22}^{min}h_{22}^{min} & \dots & \delta_{2n}^{min}h_{2n}^{min} \\ \vdots & \vdots & \vdots & \vdots \\ \delta_{n1}^{min}h_{n1}^{min} & \delta_{n2}^{min}h_{n2}^{min} & \dots & \delta_{nn}^{min}h_{nn}^{min} \end{bmatrix}([s_2 - s_1]).$$

$$\delta_{ij}^{max}, \delta_{ij}^{min} \geq 0, \quad \delta_{ij}^{max} + \delta_{ij}^{min} = 1 \quad (31)$$

Use the canonical basis from lemma 3. Then $f(s_2) - f(s_1)$ can be written as

$$f(s_2) - f(s_1) = \left[\left(\sum_{i,j=1}^{n,n} H_{ij}^{max}\delta_{ij}^{max}\right) + \left(\sum_{i,j=1}^{n,n} H_{ij}^{min}\delta_{ij}^{min}\right)\right](s_2 - s_1), \quad \delta_{ij}^{max}, \delta_{ij}^{min} \geq 0, \quad \delta_{ij}^{max} + \delta_{ij}^{min} = 1 \quad (32)$$

where $H_{ij}^{max} = e_n(i)e_n^T(j)h_{ij}^{max}$ and $H_{ij}^{min} = e_n(i)e_n^T(j)h_{ij}^{min}$.

**The Proof of Corollary to Theorem 2**:

The proof of the Corollary follows along the same lines as the proof of theorem 2 in [17], except for the definition of the scaling factor $\bar{z}_H$ and $\bar{z}_G$.

In the general problem, if all of terms in $\partial\Phi_i/\partial x_j$ are not zero, then $\sum_{i,j=1}^{n,n}\left(\delta_{ij}^{max} + \delta_{ij}^{min}\right) = n \times n = z_H$ or if all of terms in $\partial\Psi_k/\partial x_j$ are not zero, then $\sum_{k,j=1}^{m,n}\left(\gamma_{kj}^{max} + \gamma_{kj}^{min}\right) = m \times n = z_G$ . However, if in some problem, there exist $\partial\Phi_i/\partial x_j = 0$ or $\partial\Psi_k/\partial x_j = 0$, then $\sum_{i,j=1}^{n,n}\left(\delta_{ij}^{max} + \delta_{ij}^{min}\right)$ is less than $z_H$ or $\sum_{k,j=1}^{m,n}\left(\gamma_{kj}^{max} + \gamma_{kj}^{min}\right)$ is less that $z_G$. We need to define new scaling factors, $\bar{z}_H$ and $\bar{z}_G$.

$$\sum_{i,j=1}^{n,n}\left(\delta_{ij}^{max} + \delta_{ij}^{min}\right) = n \times n - w_H = \bar{z}_H \quad (33)$$

$$\sum_{k,j=1}^{m,n}\left(\gamma_{kj}^{max} + \gamma_{kj}^{min}\right) = m \times n - w_G = \bar{z}_G \quad (34)$$

where $w_H$ is number of terms in $\partial\Phi_i/\partial x_j$ that equals zero and $w_G$ is number of terms in $\partial\Psi_k/\partial x_j$ that equals zero. Now, we use $\bar{z}_H$ and $\bar{z}_G$ instead of $z_H$ and $z_G$ to complete the proof.

## REFERENCES


[1] R. Rajamani, *Vehicle Dynamics and Control*. New York: Springer Verlag, 2005.

[2] H. E. Tseng, D. Madau, B. Ashrafi, T. Brown, and D. Recker, "The development of vehicle stability control at Ford," *IEEE/ASME Transactions on Mechatronics*, Vol. 4, No. 3, pp. 223-234, September 1999.

[3] A. T. van Zanten, "Bosch ESP systems: 5 Years of experience," *SAE Trans.*, vol. 109, no. 7, pp. 428-436, 2000.

[4] R. Daily and D. M. Bevly, "The use of GPS for vehicle stability control," *IEEE Trans. Ind. Electron.*, vol. 51, no. 2, pp. 270-277, April 2004.

[5] J. Ryu and J. C. Gerdes, "Integrating inertial sensors with GPS for vehicle dynamics control," *J. Dynam. Syst., Meas., Control*, pp. 243–254, June 2004.

[6] P. Misra and P. Enge, *Global Positioning System, Signals, Measurements and Performance.* Lincoln, MA: Ganga-Jamuna Press, 2004.

[7] "Corrsys-Datron Optical Sensors," Available: http://www.corrsys-datron.com/optical_sensors.htm,.

[8] J. Farrelly and P. Wellstead, "Estimation of vehicle lateral velocity," in *Proc. IEEE Int. Conf. Control Appl*, Dearborn, MI, Sep. 1996, pp. 552–557.

[9] A. Hac and M. D. Simpson, "Estimation of vehicle side slip angle and yaw rate," in *Proc. SAE*, 2000, Paper no. 2000-10-0696.

[10] M. Hiemer, A. V. Vietinghoff, and U. Kiencke, "Determination of the vehicle body side slip angle with non-linear observer strategies," in *Proc. SAE*, 2005, Paper no. 2005-01-0400.

[11] C. Liu and H. Peng, "A state and parameter identification scheme for linearly parameterized systems," *ASME J. Dynam. Syst., Meas. Control*, vol. 120, no. 4, pp. 524–528, December 1998.

[12] P. K. Sahoo and T. Riedel, *Mean Value Theorms and Functional Equations*, 1st ed.: World Scientific Publishing Company, 1999.

[13] K. Eriksson, D. Estep, and C. Johnson, *Applied Mathematics: Body and Soul.*: Springer Berlin Heidelberg, 2010.

[14] A. Zemouche, M. Boutayeb, and G.I. Bara, "Observer Design for Nonlinear Systems: An Approach Based on the Differential Mean Value Theorem," in *Proceedings of the 44th IEEE Conference on Decision and Control*, and the 2005 European Control Conference, Seville, Spain, 2005.

[15] "*RT3000 Inertial and Measurement System User Manual*," Oxford Technical Solutions, 2004.

[16] R. Rajamani, D. Piyabongkarn, J.Y. Lew, K. Yi and G. Phanomchoeng, "Tire Road Friction Coefficient Estimation – Real-Time Estimation Methods for Active Automotive Safety Applications," *IEEE Control Systems Magazine*, Vol. 30, Issue 4, pp. 54-69, August 2010.

[17] G. Phanomchoeng, R. Rajamani, and D. Piyabongkarn, "Nonlinear Observer for Bounded Jacobian Systems, with Applications to Automotive Slip Angle Estimation", *IEEE Transactions on Automatic Control*, Issue 5, Vol. 56, May 2011.